Shear-bending interaction strength of locally buckled I-sections

M. El Aghoury

Department of Structural Engineering, Ain Shams University, El-Sarayat Street, Abbassia, P.O. Box 11517, Egypt

M. T. Hanna*

Department of Structure and Metallic Construction, Housing and Building Research Center, 87 El-Tahreer Street, Dokki, P.O. Box 1770, Egypt

Abstract. In slender sections there is a substantial post-buckling strength provided after the formation of local buckling waves. These waves happened due to normal stresses or shear stresses or both. In this study, a numerical investigation of the behavior of slender I-section beams in combined pure bending and shear has been described. The studied cases were assumed to be prevented from lateral torsional buckling. To achieve this aim, a finite element model that simulates the geometric and material nonlinear nature of the problem has been developed. Moreover, the initial geometric imperfections were included in the model. Different flange and web width-thickness ratios as well as web panel aspect ratios have been considered to draw complete set of interaction diagrams. Results reflect the interaction behavior between flange and web in resisting the combined action of moments and shear. In addition, the web panel aspect ratio will not significantly affect the combined ultimate shear-bending strength as well as the post local buckling strength gained by the section. Results are compared with that predicted by both the Eurocode 3 and the American Iron and Steel specifications, AISI–2001. Finally, an empirical interaction equation has been proposed.

Keywords : steel; stability; bending; shear; strength; local buckling.

1. Introduction

The capacity of beams subjected to transverse loads is the combination of shear and bending strengths which depend on the type of sections from which these beams are constructed. Recently steel sections are classified into compact sections that sustain full plastic moments, *Mp*, without suffering local buckling in their plate elements, non-compact sections which also resist local buckling until the most stressed point in the section reaches the yield stress but local buckling might happen before the full yielding of the section, and slender sections in which local buckling occurred in the early elastic stages of loading. Generally, in slender sections after local buckling has happened the section can still carry loads up to failure depending mainly upon the width-thickness ratios of the plate elements comprising the section and also to their boundary conditions as well as the loading type. This phenomenon is called the post-local buckling strength gained by the section. This classification is according to the flexural strength of the section. When the beams are transversally loaded local buckling waves would develop due to the shear stresses in addition to the normal stresses. Specifications allow for the presence of post local buckling due to normal

---

*Corresponding author, E-mail: m-tawfick2003@yahoo,com

stresses by applying the effective width concept. However, The post local shear buckling strength is restricted in some specifications to the beams with sufficient transverse stiffeners having relatively small web panel aspect ratios to ensure the formation of the diagonal tension field, while the other specifications neglect it. Moreover, the interaction curves between shear and bending moments are mainly based on the assumption that the web resists only the shear and that the flanges are required to resist the moments which is relevant for compact or non-compact sections. However, for beams having slender web and flanges the whole section is participating in resisting the combined acting moment and shear.

Extensive studies were made on the flexural capacity of beams fabricated from sections having relatively thin elements. Cherry (1960) presented experimental and analytical study for beams in uniform bending whose compression flanges had buckled locally. Bradford *et al*. (1984) used the non-linear finite strip method of analysis to provide an accurate solution alternative to the Winter's (1968) effective width formula. Schafer (2002) introduced the direct strength method that determines the reduced strength of cold formed beams such as channels, z, rack, and hat sections. Salem *et al*. (2005) presented an empirical equation that determines the ultimate bending moments of beams formed of slender I-sections directly using the full section properties. It takes into consideration the different modes of failure whether local, local-overall or overall. In parallel, several researchers presented analytical and experimental investigations for the strength of plate girders in shear. Basler (1961) derived an equation to determine the ultimate shear capacity of plate girders considering the tension field action that occurred after buckling of the web. The equation dos not account for the effect of the flange stiffness. Rockey and Skaloud (1972) conducted experiments on different girder models showing the effect of the flange stiffness on the ultimate shear capacity. Porter *et al*. (1975) postulated a collapse mechanism that allows for the presence of plastic hinges in the flanges. Lee and Yoo (1998) showed that the post shear buckling strength of web panels is slightly affected by the stiffness of the flanges. Although a lot of researchers studied the effect of post local buckling of slender section beams explicitly, the papers that present the combined effect of shear and moment are limited. Basler (1961) drew an interaction diagram between bending and shears strength of plate girder. He assumed that the shear strength of the section will not be affected by the presence of the applied moments unless they are higher than that are carried by the flanges only, providing that the flanges are proportioned and laterally stiffened such that the yield stress can be reached. Shahabian and Roberts (1999) outlined an approximate procedure for determining the elastic buckling loads of plates subjected to combinations of in-plane patch loading, compression, bending and shear. They used the method in obtaining interaction formulas for different combinations of loading. Roberts and Shahabian (2001) conducted experiments on series of I-section girders to determine the ultimate resistance of slender web panels to combinations of bending, shear, and patch loading. The sections they studied comprise mainly of relatively thick flanges and thin webs. Hoglund (1997) listed an interaction equation similar to that presented by Basler (1961) but it allows for the reduction in the shear resistance carried by the flanges when the applied moments are lower than that carried by the flanges.

The interaction behavior of slender I-sections subjected to combined bending and shear forces are presented in this study. In addition, the effect of large web panel aspect ratios is included. The interaction equations implemented in the Eurocode 3, (2005) and the American specifications, AISI (2001), are compared with the results of the study to examine the reliability of using these equations when designing such sections.

2. Parametric study

Earliest studies show that the bending and shear strengths of slender sections are influenced by the

width-thickness ratios of the plate elements forming the section and the aspect ratios of the web panels in addition to the end boundary conditions. Therefore the dimensions of the beams are chosen in a way that covers these factors. Four sections with flange width-thickness ratios, $b_f/2t_f$, of 20 & 30 and web width-thickness ratios, H_w/t_w, of 120 and 200 have been chosen. In addition two beam lengths, L, of 4,500 mm and 8,000 mm have been studied to account for the effect of web panel aspect ratios. Thus the web panel aspect ratios, a/H_w, are 2.25, 3.75, 4, 6.67. The beams are subjected to pure shear and pure bending as shown in Fig. 1. Beams are supported laterally so that they bent only in the plane of the web about the major axis "X-axis", and the lateral torsional buckling is prevented. Dimensions of the beams are given in Table 1.

3. Numerical model

Half of the beams are modeled as shown in Fig. 2. They are discretized using an isoparametric 4 nodes shell element (shell 4t) that is available in COSMOS/M computer program. The element has six degrees of freedom per node and accounts for the bending as well as the in-plane deformations. Formulation of this element allows for both geometric and material nonlinearities. Salem *et al.* (2007) used this element frequently with high degree of accuracy in studying similar problems such as the bi-axial behavior of slender I-section columns. In the present study, the mesh density is chosen so that the element aspect ratio is nearly equal to one. The boundary conditions on all edges of the isolated model are given in Table 2. These boundary conditions simulate the hinge and roller support of the beams, and allow the flanges to warp freely. The thickness of the first row of elements in the flanges which are subjected to the applied loads is equal to 30 mm. This is to avoid stress concentration and crippling in these parts of the beam as well as to ensure that the internal stresses due to applied loads are distributed properly all over the beam cross section.

The structural steel is modeled as an isotropic material with a von-Mises yield surface and with isotropic hardening. Young's modulus is set to 210 GPa and Poisson's ratio to 0.3. The yield stress is taken equal to 240 MPa. The material curve is assumed to be elastic perfect plastic. Salem *et al.* (2004) found that the ultimate strength is sensitive to overall geometric imperfections rather than the local geometric imperfections. Therefore, overall geometric imperfections are considered in the model by assuming the members bend in a half sine wave about the minor axis (Y-axis) with a maximum value of $L/1000$ at the beam mid-length ($L/2$). Residual stresses are not included in the model.
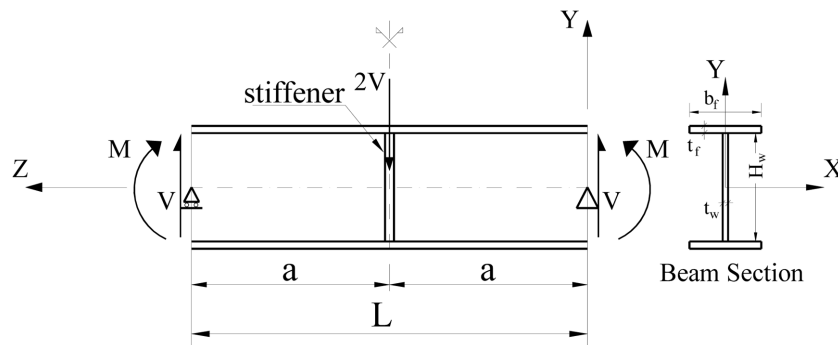

Fig. 1 Physical model

Table 1 Geometric dimensions of the studied beams

Beam No.	L (mm)	a (mm)	b_f (mm)	t_f (mm)	H_w (mm)	t_w (mm)	$b_f/2t_f$	H_w/t_w	a/H_w
1	4500	2250	200	5	600	5	20	120	3.75
2	4500	2250	200	5	1000	5	20	200	2.25
3	4500	2250	300	5	600	5	30	120	3.75
4	4500	2250	300	5	1000	5	30	200	2.25
5	8000	4000	200	5	600	5	20	120	6.67
6	8000	4000	200	5	1000	5	20	200	4
7	8000	4000	300	5	600	5	30	120	6.67
8	8000	4000	300	5	1000	5	30	200	4

(a) Axis and edges number
of the numcrical model

(b) Finite element mesh
of half of the model

Fig. 2 Finite element model

Table 2 Boundary conditions used for the 3D model

Edges	u	v	W	θ_x	θ_y	θ_z
1 (web vertical side)	0	0	1	1	0	0
2 (web vertical side)	1	1	0	0	0	1
3,4 (web-flange intersections lines)	1	0	0	0	1	0
5,6 (top and bottom flange edges)	0	0	0	0	0	1
7,8 (top and bottom flange edges)	0	0	1	1	1	0

Note : u, v, w are translations; θ_x, θ_y, θ_z are rotations in the X, Y, and Z directions, respectively, 0 denotes free and 1 denotes restrained DOF

4. Nonlinear analysis

Load control technique is used to control the increment of the external loads according to the defined time curve. Newton-Raphson iterative technique along with the tangential stiffness matrix is implemented to solve the set of non-linear equations at each load increment. Failure load is defined as the load at which the slope of the tangential stiffness matrix becomes nearly zero.

The present finite element model is verified with respect to the experimental ultimate loads obtained by Roberts and Shahabian (2001). They conducted tests on three panel I-sections girder group having non-compact flanges and slender webs. One end panel of the tested girders was subjected to a conventional shear test. During the test the adjacent panels were strengthened by welding stiffeners across the panel diagonals. To simulate the actual conditions of the test the finite element model is loaded by a concentrated load distributed at one edge as shown in Fig. 3. Table 3 summarizes the dimensions of the tested girders, the experimental results, and the numerical finite element results. It is seen that the present model can predict the ultimate strengths of the tested girders with an accuracy of ±10%.

5. Ultimate combined shear-bending strengths

The model is subjected to shear forces and uniform bending moments as shown in Fig. 4. The shear forces are distributed along the web height at one end section, the nodes that are restricted in the Y-direction at the opposite section will carry the same forces but in the reverse direction. To maintain equilibrium and to simulate the case of pure shear two forces of magnitude (Va / d) are distributed on the lines of intersection between flanges and web. In addition, forces that cause bending moments are distributed on the upper and lower flanges. The shear and normal stresses distributions across the model mid section ($a/2$) are drawn in Fig. 5 for section having b_f / $2t_f$ = 30, H_w / t_w = 200, and a/H_w = 2.25 for loads prior to local buckling and at ultimate. At loads lower than that cause local buckling in the section plate elements, the shear stress distribution is uniform throughout the web and the normal stresses distribution due to bending moments are linearly varied across the web. After local buckling waves occurred,

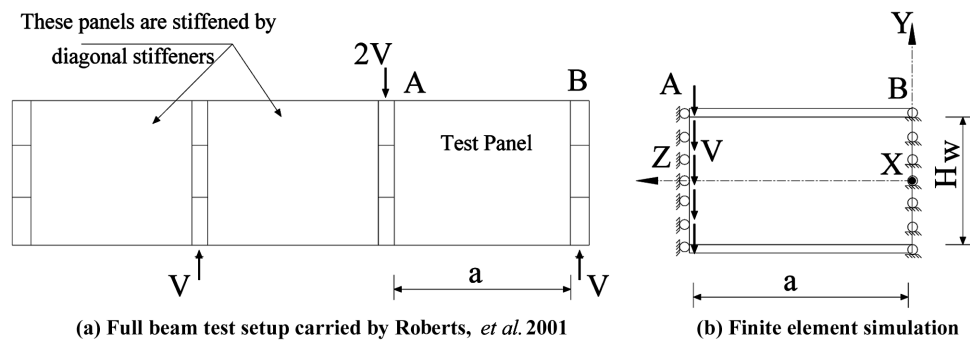(a) Full beam test setup carried by Roberts, *et al.* 2001   (b) Finite element simulation

Fig. 3 Slender plate girders tested by Roberts, *et al*, (2001) and the corresponding finite element simulation

Table 3 Comparison between the tests results (Roberts, *et al.* 2001) and the F.E.M. results

Specimen	b_f/ $2t_f$	H_w / t_w	a / H_w	EXP. results		F.E.M. results		$\dfrac{V_{Uexp.}}{V_{uF.E.M}}$
				V_u (kN)	M_u (KN.m)	V_u (kN)	M_u (KN.m)	
PG1	8	146.1	1.0	373	227	352.5	211.5	1.058
PG2	14.7	290.32	1.0	271	245	291.8	262.6	0.928
PG3	9.8	187.5	1.5	202	182	185.1	166.6	1.091
PG4	10.1	263.15	2.0	87	87	79.7	79.7	1.091
PG5	7.28	198.01	1.0	160	97	146.6	87.96	1.091

a) Loading pattern

b) Time curve of the pure shear loads
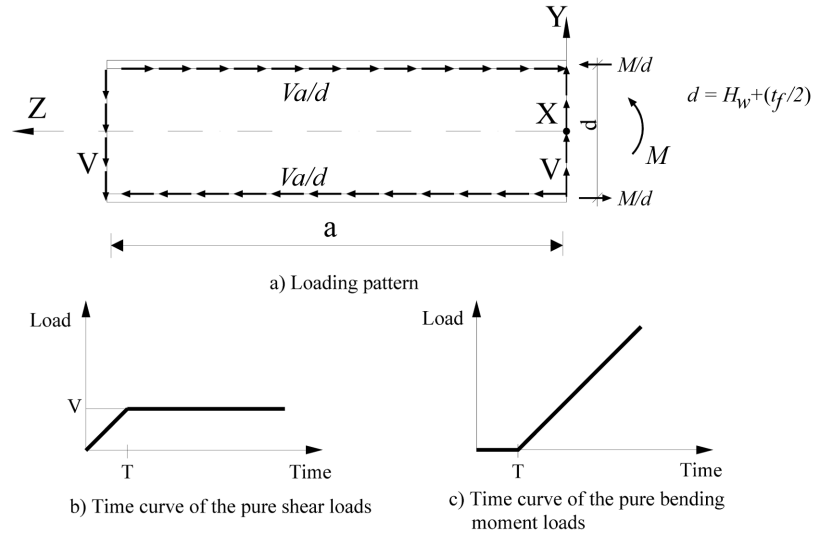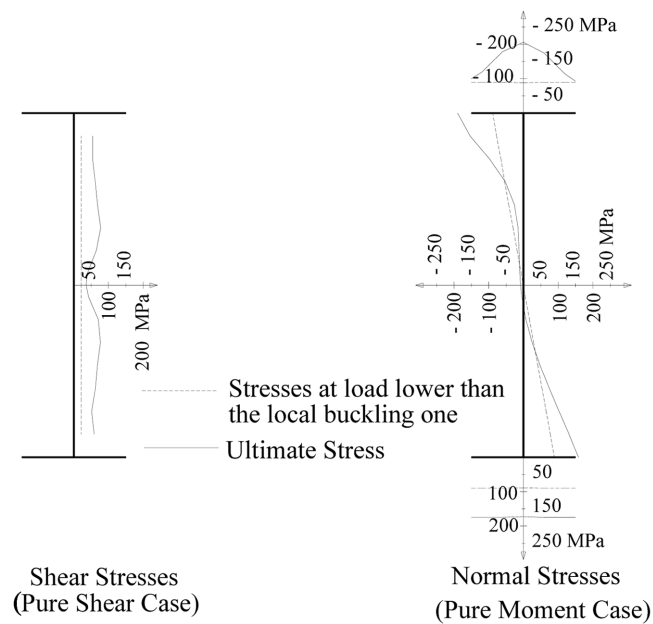
c) Time curve of the pure bending moment loads

Fig. 4 Loading simulation on the finite element model

shear as well as normal stresses distributions become nonlinear across the section. This reflects that shear and normal stresses are accurately distributed in this model and under these loading arrangements.

Loads are applied on the model sequentially, shear forces were applied first from zero to a certain value, this value is kept constant then the end bending moments are increased from zero to the ultimate value. Time curves of the shear and the bending moments are shown in Fig. 4.

By examining the failure modes of the beams it is observed that when beams are loaded in pure shear

Shear Stresses (Pure Shear Case)

Normal Stresses (Pure Moment Case)

Fig. 5 Model mid section (*a*/2) stress distribution

the failure mode consists of series of skewed local buckling waves in the web as presented in Fig. 6(a). Moreover, the number of shear buckling waves occurred depending mainly on the web panel aspect ratios, a / H_w, regardless the flange width thickness ratios. For web panel aspect ratio, $a/H_w = 2.25$ and $b_f / 2t_f = 20$ & 30 one wave is formed in the web, whereas for aspect ratios, $a / H_w = 6$ and $b_f / 2t_f = 20$ & 30 two waves occurred in the web panel. Due to the interaction between the flange and web, the flanges rotated as a result of out of plane rotation of the web. In addition, in all cases the diagonal principal stresses do not reach the yield stress. Fore beams that are loaded in pure bending moments the failure modes are as shown in Fig. 6(b), which consists of longitudinal local buckling waves in the web and flanges. However, beams with $b_f / 2t_f = 20$ and $H_w / t_w = 120$ there are no local buckling waves happened. Also, the longitudinal stresses do not reach the yield value. Fig. 6(c) shows the failure mode of the beam due to the combined effect of bending and shear. The number of waves in the web depends on the flange width-thickness ratios and the web panel aspect ratios.

Fig. 7 illustrates the variation of the ultimate shear as well as ultimate normal stress distributions across section having $b_f / 2t_f = 30$, $H_w / t_w = 200$, and $a / H_w = 2.25$ due to the presence of different ratios of end moments, M_u / M_{uo}, and shear forces, V_u / V_{uo}, respectively. The ratios are taken as 0.0, 0.25, 0.5, and 0.75. The value zero represents the case of pure shear and pure moment. It is found that the pure shear local buckling waves commences at approximately half the ultimate shear capacity of the section, while the local buckling waves due to pure bending moments starts nearly at three quarters the ultimate moment capacity.

By comparing the normal stress distribution corresponding to different shear load ratios; it can be seen that the presence of shear loads results in shifting the position of the neutral axis towards the compression side and consequantly reduces the moment capacity. Moreover, for shear load ratios $V_u / V_{uo} = 0$, 0.25 where there are no local shear buckling waves this shift is minor. However, a considreble shift in the location of the neutral axis can be noticed when $V_u / V_{uo} \geq 0.5$ (i.e. shear local buckling occurred) leading to big reduction in the critical moment capacity of the section. In addition, the ultimate normal stress on the flanges decreases as the shear load ratio increases.

The shear stress distribution is nonlinear for the cases where there are no local buckling waves due to moments, $M_u / M_{uo} = 0$, 0.25, 0.5. On the other hand, in the case where these waves are present, $M_u / M_{uo} = 0.75$, it becomes almost uniform over the web. Also, Fig. 7 reflects that the shear stress distribution reduces due to the presence of normal stress distribution.
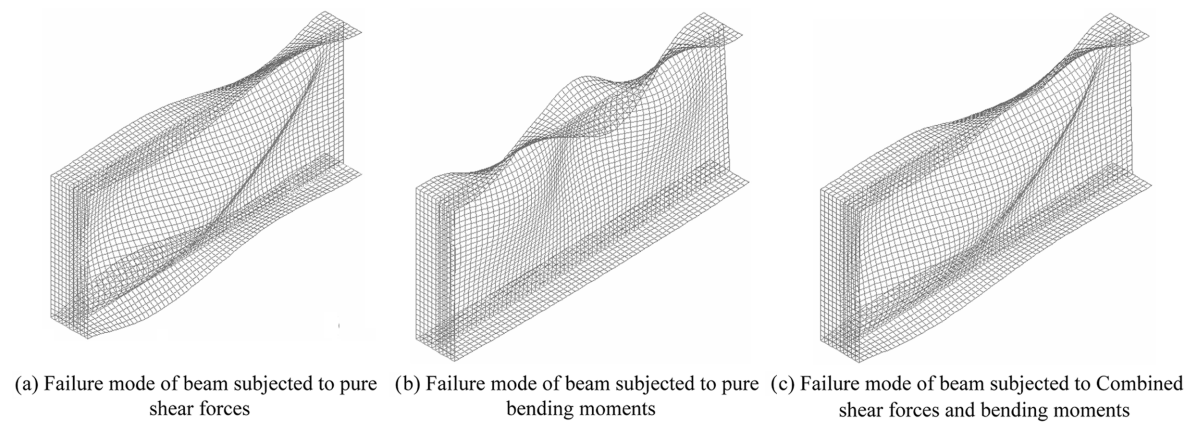

(a) Failure mode of beam subjected to pure shear forces (b) Failure mode of beam subjected to pure bending moments (c) Failure mode of beam subjected to Combined shear forces and bending moments
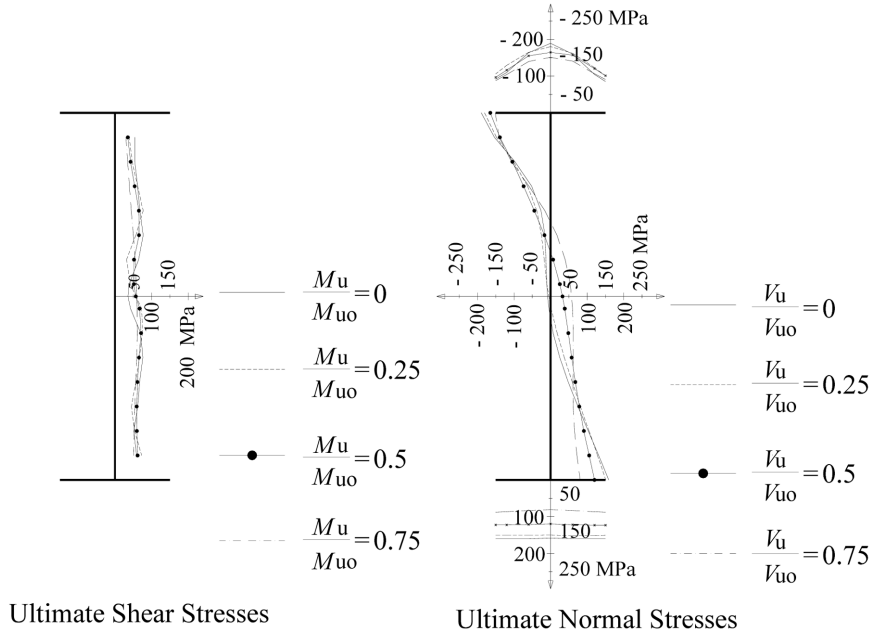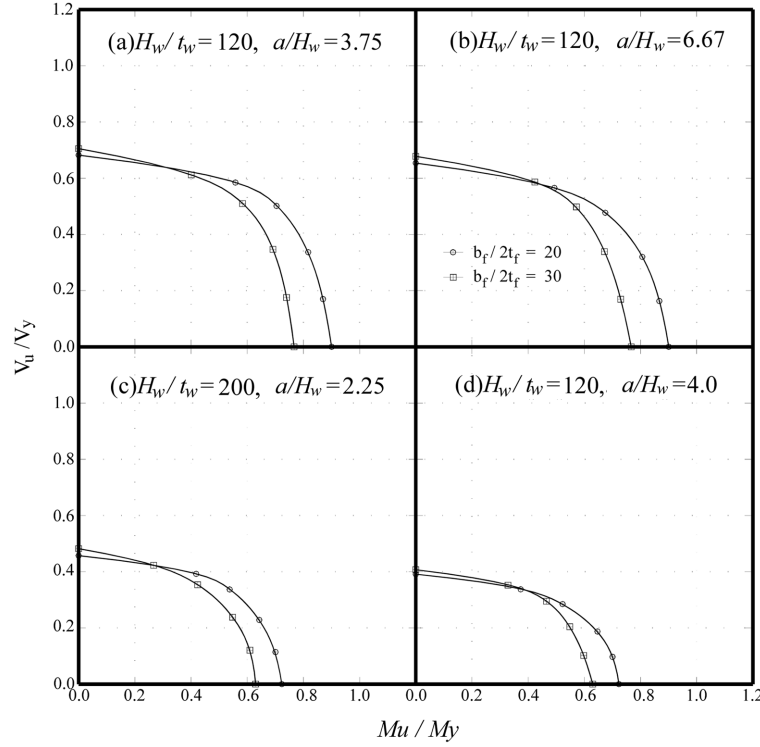
Fig. 6 Different failure modes

Fig. 7 Model mid section (a/2) stress distribution at different bending and shear combinations

6. Shear–bending interaction diagrams

The shear-bending interaction curves in normalized form have been plotted for beams with different flange and web width-thickness ratios as well as web panel aspect ratios. Results are shown in Fig. 8 where the ultimate shear forces, V_u, has been normalized with respect to the yield shear forces, V_y, which cause full yielding to the web ($0.577 \times F_y \times A_w$, F_y = yield stress, A_w = area of the web = $H_w \times t_w$) and the ultimate moments, M_u, has been normalized with respect to the first yield moments that cause yielding in the flanges, M_y. Fig. 8 reflects that both the shear and bending strengths of the sections are sensitive to the presence of the combined moments and shear forces. In spite of the reduction in the shear strengths are low for small ratios of applied moments, $M_u / M_y < 0.4$ the bending strengths noticeably reduced due to small values of shear forces, $V_u / V_y < 0.2$. In addition, increasing the web and flange width-thickness ratio decreases the combined shear-bending strengths. However, the flange width-thickness ratios have no significant effect on the combined strengths for lower ratio of moment to shear. Furthermore, changing the web panel aspect ratio, a/H_w, will not significantly affect the combined shear-bending strength of the sections.

7. Combined post-local buckling reserve capacity

Sections having thin elements exhibits considerable postbuckling strength after elastic buckling waves occurred. To study this reserve strength, the ultimate combined shear, V_u, and bending, M_u, strengths are normalized with respect to the elastic buckling loads of the cases where the beams are loaded only by shear, V_{cr}, and only by moments, M_{cr}. The elastic buckling loads V_{cr} and M_{cr} are determined by the eigenvalue analysis provided by COSMOS/M package. The normalized ratios are shown in Fig. 9. For
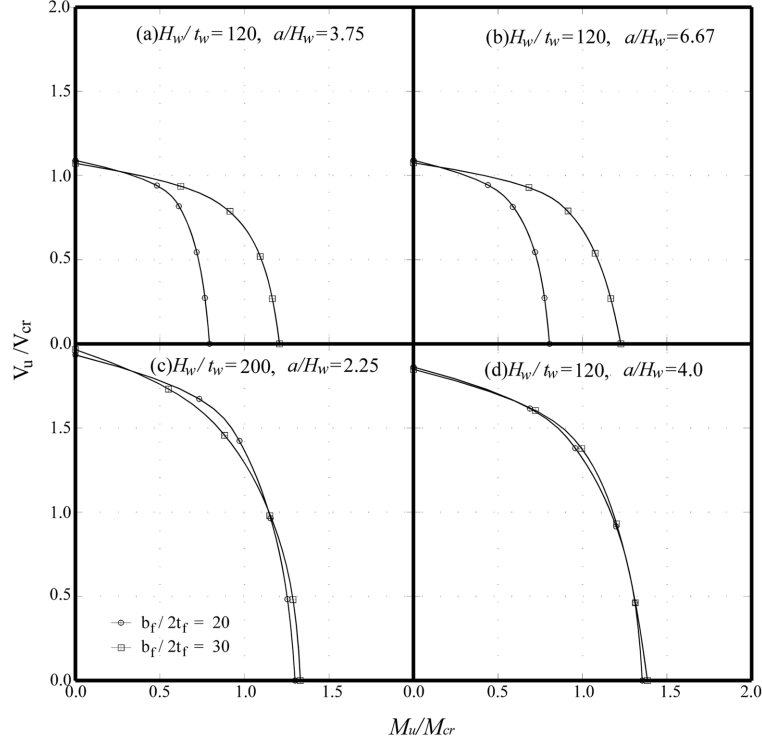
Fig. 8 V_u/V_y versus M_u/M_y

small values of web width-thickness ratios, $H_w / t_w = 120$, the post local buckling strength gained by the section is mainly affected by the flange width-thickness ratios, $b_f / 2t_f$, when the beams are loaded mainly by bending moments. However, when the shear stresses increase, the post local buckling strength becomes very small (less than 10%). However, for slender web width-thickness ratios, $H_w / t_w = 200$, the post local buckling strength gained by the section has not been affected by the flange width-thickness ratios. In addition it becomes effective when the beams are loaded mainly by shear forces, about 80%, than that when loaded by bending moments, about 40%. Moreover, the web panel aspect ratio has no effect on the post local buckling gained by the section.

To conclude, the web width-thickness ratios is the dominant parameter that influences the combined shear-bending strengths as well as the post-local buckling strength gained by the section.

8. Comparison with design strengths

The ultimate finite element shear-bending interaction curves have been compared with the unfactored design strengths predicted in the Eurocode 3 and the North American specification for the design of steel structures, AISI-2001. The Eurocode 3 has adopted the combined bending and shear Eq. (1). The code limits the uses of this equation when the applied shear force, V, is higher than half the ultimate shear resistance of the section, V_{uo}, and also the applied moment, M, is higher than the moment capacity of the flanges, M_f. It assumes that stresses in the web which are caused be bending moments do not influence the

Fig. 9 V_u/V_{cr} versus M_u/M_{cr}

shear resistance of the section provided that the applied moments are smaller than the moment capacity of the flanges. On the other hand the moment capacity of the section will not be affected by the presence of the shear force unless the applied shear force is higher than half the ultimate shear resistance of the section. AISI-2001 defines two interaction equations for the combined bending and shear. One for beams with unreinforcied web, Eq. (2), and the other equation is for beams with transverse web stiffeners, Eq. (3).

$$\frac{M}{M_{uo}} + \left(1 - \frac{M_f}{M_{uo}}\right)\left(2\frac{V}{V_{uo}} - 1\right)^2 \leq 1 \tag{1}$$

$$\left(\frac{M}{M_{uo}}\right)^2 + \left(\frac{V}{V_{uo}}\right)^2 \leq 1 \tag{2}$$

$$0.6\left(\frac{M}{M_{uo}}\right) + \left(\frac{V}{V_{uo}}\right) \leq 1.3 \tag{3}$$

Generally, in both codes the ultimate shear strength has been calculated using the full section

properties based on the web width-thickness ratio, and the web panel aspect ratio. Eurocode 3 divided the section into flanges and web. The contribution of the web to shear resistance depends on the rigidity of the beam end. There are three cases defined by the code which are: 1) no end post, 2) rigid end post which comprises of two double-sided transverse stiffeners that form the flanges of a short beam of length H_w, and 3) non-rigid end post that may be a single double sided stiffeners. Case 3 has been considered when determining the shear resistance of the section in this study. However, the North American specifications, AISI-2001, does not give any restriction to the nature of the beam ends. Moreover, it neglects the contribution of the flanges. In addition, the ultimate moments have been calculated using the effective width concept in both the AISI-2001 and Eurocode 3.

For the purpose of comparison, numerical strengths and design strengths have been normalized with respect to the ultimate strengths obtained by the finite element analysis for the pure shear case, V_{uo}, and the pure bending case, M_{uo}. The relations between the ratios V_u/V_{uo} and M_u/M_{uo} were plotted in Fig. 10 for I-sections having $b_f/2t_f$ = 20 & 30, H_w/t_w = 120 & 200, a/H_w = 3.75 & 4. Comparison shows that both the Eurocode 3 and the North American specification, AISI-2001, conservatively predict the combined bending and shear strengths for the cases having small web width-thickness ratios, H_w/t_w = 120. For the cases having large web width-thickness ratios, H_w/t_w = 200, the European code prediction is very close to that of the finite element results. However, it becomes slightly overestimate the design strengths at moderate ratio of moment to shear for I-sections having H_w/t_w = 200, $b_f/2t_f$ = 20, a/H_w = 4. Controversially, the North American specifications, AISI-2001, underestimate the strengths especially when the beams are mainly loaded by shear forces. Because the effect of the post local shear buckling strength is ignored in the design equations.

9. Suggested interaction equation

The numerical finite element results are used to derive an empirical equation accounts for the accurate behavior of slender I-section beams in combined bending and shear. This equation should combine the ratios of the applied forces to the strengths of the section. Therefore, the proposed Eq. (4) is used to fit the finite element results. It is found that when m = 2 and n = 3 give better correlation with the finite element results as shown in Fig. 11 for cases having H_w/t_w = 120 &200, $b_f/2t_f$ = 20&30, a = 3.75 & 4. It is evident that the difference between the finite element results and that of the proposed equation is within ±8%.

$$\left(\frac{V_u}{V_{uo}}\right)^m + \left(\frac{M_u}{M_{uo}}\right)^n \leq 1 \tag{4}$$

The proposed interaction equation is plotted along with the experimental results as well as the equations listed in Roberts *et al.* (2001) (Eq. 5) and Hoglund (1997) (Eq. 6) in Fig. 12. Eq. (5) slightly underestimates the combined shear-bending strengths for the cases subjected to moderate shear to moment ratio. However, it matches well with Eq. (4) when the beams are loaded mainly in shear. Equation 6 consists of two parts. The first part represent the case where the girder subjected to moments of small magnitudes ($M < M_f$) then the stresses in the web that are caused by bending moments do not influence that portion of the shear stresses resisted by the web, and reducing only the portion resisted by the flanges. In the second part where $M > M_f$ then the flanges can not contribute to the shear capacity of the girder, and the capacity of the web to carry shear forces is reduced. The second part of Eq. (6) is similar
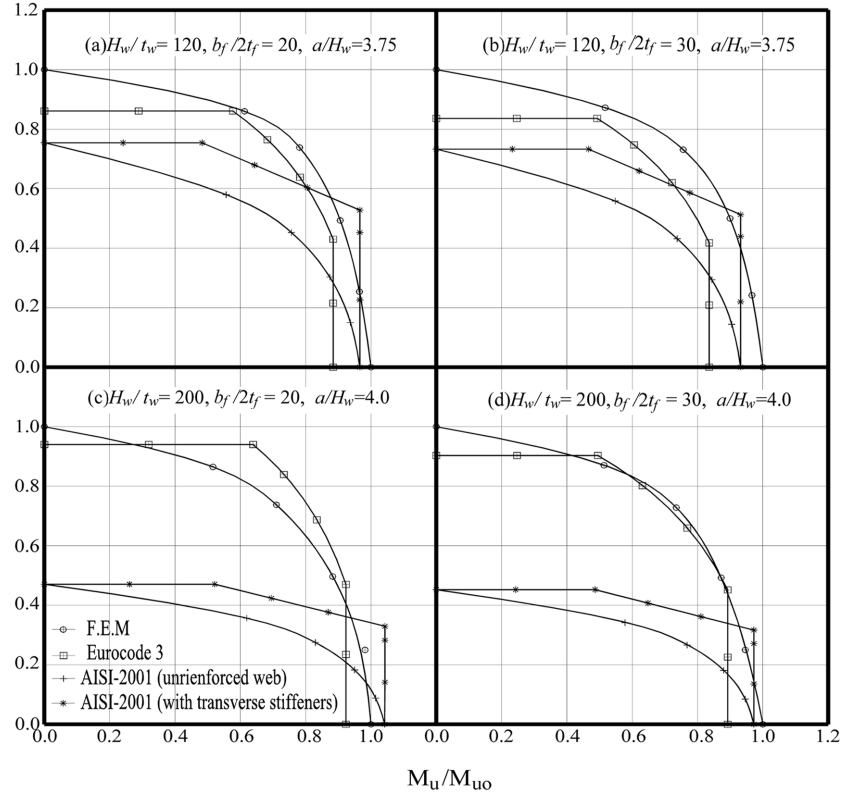
Fig. 10 Comparison between F.E.M. and different standard codes combined shear-bending strengths

to that proposed by Basler (1961).

It is evident that the proposed interaction equation (Eq. 4) is closer to that presented by Hoglund (1997). However, Hoglund (1997) is a bit higher in the range when the beams subjected to high shear force and small magnitudes of bending moments. In addition the experimental results in Roberts *et al.* (2001) are very close to that predicted by Eq. (6).

$$\left(\frac{V_u}{V_{uo}}\right) + \left(\frac{M_u}{M_{uo}}\right)^4 \leq 1 \tag{5}$$

$$\begin{aligned} V_{red} &= V_w + V_f\left(1 - \left(\frac{M}{M_f}\right)^2\right) & M < M_f \\ M &= M_f + (M_P - M_f)\left(1 - \left(\frac{V}{V_w}\right)^2\right) & M > M_f \end{aligned} \tag{6}$$

10. Conclusions

The influence of the flange and web width-thickness ratios as well as the web panel aspect ratios on
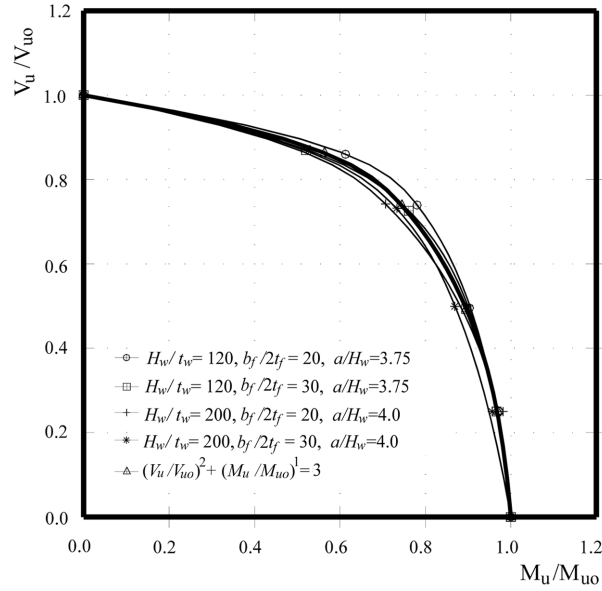
Fig. 11 Comparison between F.E.M. and proposed equation for combined shear-bending strengths
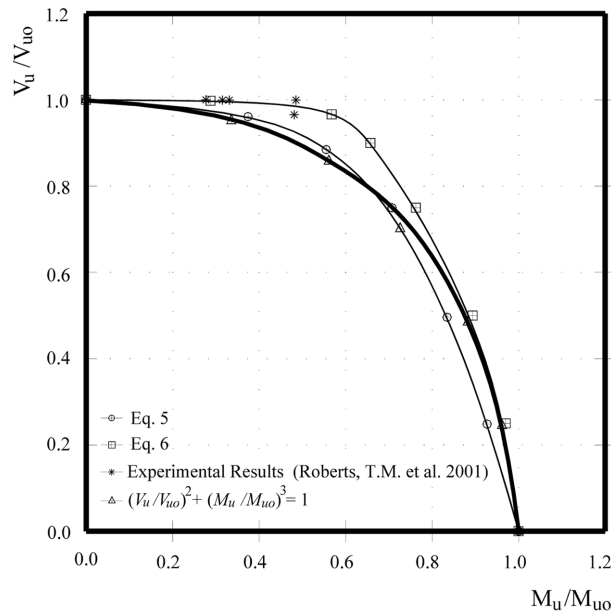

Fig. 12 Comparison between the proposed equation and the pre-published results

the ultimate shear-bending interaction capacity of locally buckled I-sections have been introduced in this research. The parameters cover range of large web panel aspect ratios. The strengths are obtained numerically by a nonlinear finite element model. The model is capable to simulate the accurate geometric and material nonlinear nature of the problem. The finite element model results are verified by comparing

them with pre-published experimental results. Results show that there are an interaction between the flange slenderness and web slenderness in resisting the combined strengths. Moreover, the shear and bending strengths are affected by the presence of the coupled stresses even for small percent. In addition, both the Eurocode 3 and the North American specifications, AISI 2001, underestimate the combined shear-bending strengths for small web slenderness ratio. However, for higher web width-thickness ratios the Eurocode 3 become a bit unconservative. Lastly, an empirical interaction equation has been suggested. This equation accurately predicts the shear bending strengths of slender web and flanges I-sections.

References

AISI (2001), *North American Specification for the Design of Cold-Formed Steel Structural Members*.

Basler, K. (1961), "Strength of plate girders in shear", *J. Struct Div, ASCE,* **87**(7),151-180.

Basler, K. (1961), "Strength of plate girders in combined bending and shear", *J. Strucrt. Div, ASCE,* **87**(7),181-197.

Bradford, M. A. and Hancock, G. J. (1984), "Elastic interaction of local and lateral buckling in beams", *Thin-Walled Struct.,* **2**(1), p.1-25.

Cherry, S. (1960), "The stability of beams with buckled compression flanges", *Struct. Eng.,* **38**(9), 277-85.

Eurocode 3, prEN 1993. (2005), Design of Steel Structures, Part 1-5: Strength and stability of planar plated structures without transverse loading.

Hoglund, T. (1997), " Shear buckling resistance of steel and aluminium plate girders", *Thin-Walled Struct.* **29**,13-30.

Lee, S. C. and Yoo, C. H. (1998), "Strength of plate girder web panels under pure shear", *J. Struct. Eng ASCE,* **124**(2),184–194.

Porter, D.M., Rockey, K.C. and Evans, H.R. (1975), "The collapse behaviour of plate girders loaded in shear", *The Struct. Eng.,* **53** (8),313-325.

Roberts, T.M. and Shahabian, F. (2001), "Ultimate resistance of slender web panels to combined bending shear and patch loading", *J. Constr. Steel Res.* **57**,779-790.

Rockey, K.C. and Skaloud, M. (1972), "The Ultimate load behaviour of plate girders loaded in shear", *The Struct Eng.,* **50**(1),.29-47.

Salem, A.H., El Aghoury, M., El Dib, F.F. and Hanna, M.T. (2004), "Ultimate capacity of I-slender section columns", *J. Constr. Steel Res,* **60**, 1193-1211.

Salem, A.H., El Aghoury, M., El Dib, F.F. and Hanna, M.T. (2005). "Strength of slender I-section beams", *4th European conference on steel and composite structures, Eurosteel 2005,* Maastricht, The Netherlands, June.

Salem, A.H., El Aghoury, M., El Dib, F.F. and Hanna, M.T. (2007), "Strength of biaxially loaded slender I-section beam-columns", *Can. J. Civ. Eng.,* **34**, (2), 219–227.

Schafer, B.W. (2002), "Design manual for the direct strength method of cold-formed steel design", Final Report to the American Iron and Steel Institute, Washington, D.C.

Shahabian, F. and Roberts, T.M. (1999), "Buckling of slender web plates subjected to combinations of in plane loading", *J. Constr. Steel Res.,* **51**,1-19.

Winter, G. (1968), "Thin walled structures–theoretical solutions and test results", *Eighth Congress,* IABSE.

DN